THE JOURNAL OF BIOLOGICAL CHEMISTRY VOL. 284, NO. 28, pp. 18715–18725, July 10, 2009

The C Terminus of Na^+,K^+-ATPase Controls Na^+ Affinity on Both Sides of the Membrane through Arg^{935}*[S]◆

Received for publication, March 23, 2009, and in revised form, April 29, 2009 Published, JBC Papers in Press, May 5, 2009, DOI 10.1074/jbc.M109.015099

Mads S. Toustrup-Jensen[‡§], Rikke Holm[‡§], Anja Pernille Einholm[‡§], Vivien Rodacker Schack[‡§], J. Preben Morth[‡¶], Poul Nissen[‡¶], Jens Peter Andersen[‡§], and Bente Vilsen[‡§1]

From the [‡]Centre for Membrane Pumps in Cells and Disease – PUMPKIN, Danish National Research Foundation and the Departments of [§]Physiology and Biophysics and [¶]Molecular Biology, Aarhus University, DK-8000 Aarhus C, Denmark

The Na^+,K^+-ATPase C terminus has a unique location between transmembrane segments, appearing to participate in a network of interactions. We have examined the functional consequences of amino acid substitutions in this region and deletions of the C terminus of varying lengths. Assays revealing separately the mutational effects on internally and externally facing Na^+ sites, as well as E_1-E_2 conformational changes, have been applied. The results pinpoint the two terminal tyrosines, Tyr^{1017} and Tyr^{1018}, as well as putative interaction partners, Arg^{935} in the loop between transmembrane segments M8 and M9 and Lys^{768} in transmembrane segment M5, as crucial to Na^+ activation of phosphorylation of E_1, a partial reaction reflecting Na^+ interaction on the cytoplasmic side of the membrane. Tyr^{1017}, Tyr^{1018}, and Arg^{935} are furthermore indispensable to Na^+ interaction on the extracellular side of the membrane, as revealed by inability of high Na^+ concentrations to drive the transition from E_1P to E_2P backwards toward E_1P and inhibit Na^+-ATPase activity in mutants. Lys^{768} is not important for Na^+ binding from the external side of the membrane but is involved in stabilization of the E_2 form. These data demonstrate that the C terminus controls Na^+ affinity on both sides of the membrane and suggest that Arg^{935} constitutes an important link between the C terminus and the third Na^+ site, involving an arginine-π stacking interaction between Arg^{935} and the C-terminal tyrosines. Lys^{768} may interact preferentially with the C terminus in E_1 and E_1P forms and with the loop between transmembrane segments M6 and M7 in E_2 and E_2P forms.

The Na^+,K^+-ATPase is a membrane-bound ion pump that uses energy liberated by hydrolysis of ATP to exchange intracellular Na^+ for extracellular K^+ at a ratio of 3:2, thus creating the gradients for Na^+ and K^+ across the cell membrane required for electrical excitability, cellular uptake of ions, nutrients, and neurotransmitters, and regulation of cell volume and intracellular pH (1, 2). Like other P-type ATPases, such as the Ca^{2+}-ATPase and H^+,K^+-ATPase, the Na^+,K^+-ATPase forms a phosphorylated enzyme intermediate through transfer of the γ-phosphate of ATP to a conserved aspartate residue in the P-domain. It is generally believed that the transport mechanism is consecutive, the Na^+ ions being translocated before K^+. The binding of three Na^+ ions from the cytoplasmic side to the E_1 form triggers phosphorylation of the enzyme by ATP, and binding of two K^+ ions from the extracellular side to E_2P activates the dephosphorylation ("Post-Albers model," Scheme 1) (3). During transfer across the membrane, the Na^+ and K^+ ions become occluded in the binding pocket, being temporarily unable to dissociate to either side of the membrane. The three Na^+ ions are released sequentially to the external side in connection with the $E_1P \rightarrow E_2P$ conformational transition, and K^+ dissociates to the cytoplasmic side in association with the $E_2 \rightarrow E_1$ transition of the dephosphoenzyme (Scheme 1).

Recently, the structure of the Na^+,K^+-ATPase in the E_2 form with two occluded Rb^+ ions bound as K^+ congeners was determined by x-ray crystallography at 3.5 Å resolution (4). The α-subunit consists of 10 membrane-spanning helices, αM1–αM10,[2] and three distinct cytoplasmic domains denoted A (actuator), N (nucleotide binding), and P (phosphorylation) by analogy to the closely related sarco(endo)plasmic reticulum Ca^{2+}-ATPase (SERCA) (5). The K^+ binding pocket is located between transmembrane helices αM4, αM5, αM6, and αM8. The K^+ binding sites are comprised of residues homologous to those binding the two Ca^{2+} ions in the E_1 form of the Ca^{2+}-ATPase, and it is therefore likely that they also make up two of the three Na^+ binding sites in the Na^+,K^+-ATPase E_1 form. The location of the third Na^+ site that has no counterpart in the Ca^{2+}-ATPase remains elusive (4). The Na^+,K^+-ATPase also consists of, in addition to the α-subunit, a β-subunit with a large extracellular domain and a single membrane span (βM). The β-subunit is required for routing the α-subunit to the plasma membrane and is furthermore essential for K^+ binding (6), possibly because it influences the positioning of some of the transmembrane segments of the α-subunit in E_2 conformation. In many cell types, the αβ-complex interacts with a small regulatory transmembrane protein belonging to the F*X*YD family (7). Because the Na^+ concentration in a normal cell is rather low (typically around 10–15 mM), the Na^+,K^+-ATPase operates at only a fraction of its maximal pumping rate. Hence, changes in the cytoplasmic Na^+ concentration or in the affinity for

* This study was funded in part by grants from the Lundbeck Foundation, Denmark, the Danish Medical Research Council, the Novo Nordisk Foundation (Fabrikant Vilhelm Pedersen og Hustrus Legat), Denmark, and the Danish National Research Foundation (PUMPKIN Centre).
◆ This article was selected as a Paper of the Week.
[S] The on-line version of this article (available at http://www.jbc.org) contains supplemental Figs. S1–S2.
[1] To whom correspondence should be addressed: Deptartment of Physiology and Biophysics, Aarhus University, Ole Worms Allé 6, Blg. 1180, DK-8000 Aarhus C, Denmark. Fax: 45-86129065; E-mail: bv@fi.au.dk.

[2] The abbreviations used are: αM1–αM10 or M1–M10, the 10 transmembrane segments of the α-subunit numbered from the N terminus; βM, the transmembrane segment of the β-subunit.

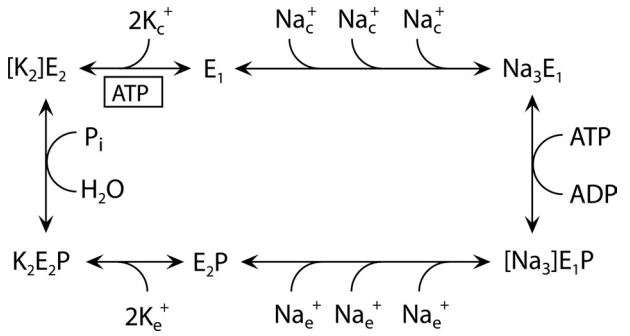

SCHEME 1. **Model for the reaction cycle of the Na^+,K^+-ATPase (Post-Albers model).** Occluded ions are shown in *brackets*. The cytoplasmic and extracellular ions binding at transport sites are indicated by the subscript *c* and *e*, respectively. ATP binding with low affinity is shown *boxed*.

Na^+ constitute important regulatory measures, and the Na^+ affinity is differentially affected by the various F*X*YD proteins.

The crystal structure of the Na^+,K^+-ATPase (4) revealed an unexpected location of the C terminus of the α-subunit between the transmembrane helices (see Fig. 1*A*). The C terminus consists of a PGG motif followed by an extension of eight residues relative to the corresponding C terminus of the Ca^{2+}-ATPase (SERCA1a isoform). The first part of this extension forms a small helix between the transmembrane helices βM, αM7, and αM10, and the two C-terminal tyrosine residues are accommodated in a binding pocket between αM7, αM8, and αM5 (see Fig. 1, *B–D*). This unique position prompted us to examine the functional role of the C terminus by deletion of the five most C-terminal residues KETYY, which reduced the Na^+ affinity of the E_1 form conspicuously, thus indicating a previously unrecognized importance of the C terminus for Na^+ binding at one or more of the three cytoplasmically facing activating sites (4). The putative role of the C terminus in regulation of Na^+ affinity led us to denote it "switch region." It was, however, not clear, whether the position of the C-terminal carboxylate group, the interaction of the side chains, or both are crucial for Na^+ binding. The C terminus and its binding pocket are well resolved in the crystal structure, as indicated by the electron density map contoured at 1σ in Fig. 1, *A* and *B*, thus providing information of considerable detail and confidence. Hence, a possible involvement of the C-terminal carboxylate group as well as the hydroxyl groups of the two C-terminal tyrosines in hydrogen/salt bridge formation is suggested (see Fig. 1, *B–D*). The terminal tyrosine residue,[3] Tyr^{1018}, seems to be in position to make bonds with Lys^{768} in M5 and Arg^{935} in the loop connecting M8 and M9, and Tyr^{1017} may also interact with Arg^{935} (Fig. 1, *B–D*). It is unknown whether these bonds suggested by the crystal structure of the E_2 form with bound Rb^+ exist in the Na^+-bound E_1 form and, if so, whether they could mediate the observed effects of the C terminus on Na^+ affinity. An important question is furthermore whether the C terminus is of any importance in relation to the Na^+ sites in the externally facing configuration in the phosphoenzyme.

To understand in detail the importance of the structural features of the C terminus, we have in this study examined the functional consequences of replacing individual amino acids in this region and introducing deletions of the C terminus of variable length. The interaction with Na^+ in the dephosphoenzyme as well as in the phosphoenzyme was studied, thus revealing separately the mutational effects on internally and externally exposed Na^+ sites.

[3] All numbering of Na^+,K^+-ATPase residues in this article refers to the sequence of the rat α_1-isoform.

EXPERIMENTAL PROCEDURES

Mutations were introduced into full-length cDNA encoding the rat kidney Na^+,K^+-ATPase (α_1-isoform) using the QuikChange site-directed mutagenesis kit (Stratagene), and the mutants and wild type were expressed in COS-1 cells, using 5 μM ouabain in the growth medium to inhibit the endogenous COS-1 cell enzyme and thereby select stable transfectants (8, 9). The presence of the desired mutations was verified by sequencing the cDNA before transfection into the COS-1 cells, and in most cases, also by sequencing the DNA stably integrated into the genome of the isolated ouabain-resistant COS-1 cell lines.

The crude plasma membrane fraction containing expressed wild-type or mutant Na^+,K^+-ATPase was isolated by differential centrifugation, and prior to functional analysis, the plasma membranes were made leaky with alamethicin or deoxycholate (8). Hence, it can be assumed that the membrane potential was zero during the measurements.

Measurements of the ATPase activity by following the release of P_i at 37 °C and phosphorylation/dephosphorylation studies using [γ-^{32}P]ATP were carried out as described previously (8, 10–12); the media compositions are detailed in the figure legends. The acid-precipitated ^{32}P-labeled phosphoenzyme was washed by centrifugation and subjected to SDS-polyacrylamide gel electrophoresis at pH 6.0 (10), and the radioactivity associated with the separated Na^+,K^+-ATPase band was quantified by "imaging" using a Packard Cyclone™ storage phosphor system. The active site concentration was determined by phosphorylation at 0 °C in the presence of 2 μM [γ-^{32}P]ATP, 3 mM Mg^{2+}, 150 mM Na^+, and oligomycin (20 μg/ml) to block dephosphorylation and thereby obtain stoichiometric phosphorylation (10). The catalytic turnover rate was calculated as the ratio between the rate of ATP hydrolysis and the active site concentration. The contribution from endogenous Na^+,K^+-ATPase in the functional assays was eliminated by including ouabain in the reaction media at a concentration sufficient to inhibit the endogenous enzyme but too low to affect the rat Na^+,K^+-ATPase.

Each data point shown is the average value corresponding to at least three independent measurements. Data normalization, averaging, and non-linear regression analysis were carried out as described previously (10, 11), and the results are reported ± S.E.

RESULTS

Mutants Studied—Seventeen new mutations to residues in the C-terminal region of the α-subunit were studied (Table 1). These mutations encompass C-terminal deletions of varying lengths ranging from one or both of the two terminal tyrosines to an eight-residue deletion including the complete C-terminal helix (WVEKE). The EKE part of the helix was also examined in

TABLE 1
Ligand concentration dependence and relative amount of E_2P

	$K_{0.5}(K^+)$[a]	$K_{0.5}(Na^+)$[b]	E_2P[c]	$K_{0.5}$(ATP)[d]	$K_{0.5}$(vanadate)[e]	$K_{0.5}$(ouabain)[f]
	μM	μM	%	μM	μM	μM
Wild type	669 ± 14	437 ± 9	57	360 ± 17	3.2 ± 0.1	158 ± 7
ΔY (del[g] Tyr^{1018})	878 ± 30	1016 ± 34	ND[h]	176 ± 9	4.3 ± 0.1	124 ± 8
ΔYY (del Tyr^{1017}–Tyr^{1018})	1021 ± 13	4059 ± 78	75	172 ± 8	3.6 ± 0.1	140 ± 11
ΔTYY (del Thr^{1016}–Tyr^{1018})	793 ± 34	7559 ± 230	68	104 ± 8	5.9 ± 0.5	195 ± 37
ΔKETYY (del Lys^{1014}–Tyr^{1018})[i]	700 ± 43	11,458 ± 637	76	114 ± 9	5.4 ± 0.3	240 ± 46
ΔWVEKETYY (del Trp^{1011}–Tyr^{1018})	695 ± 68	10,854 ± 633	85	100 ± 8	6.0 ± 0.5	255 ± 35
Y1018A	933 ± 17	2211 ± 49	ND	252 ± 12	1.8 ± 0.1	118 ± 7
Y1018F	905 ± 13	617 ± 18	ND	357 ± 37	3.3 ± 0.2	144 ± 12
Y1017A	720 ± 28	1169 ± 55	ND	272 ± 17	2.0 ± 0.1	151 ± 14
Y1017F	691 ± 12	525 ± 16	ND	388 ± 29	2.3 ± 0.1	147 ± 11
YY-AA (Y1017A/Y1018A)	555 ± 1	13,919 ± 614	70	145 ± 6	6.1 ± 0.2	276 ± 10
T1016A	814 ± 27	582 ± 25	ND	294 ± 11	5.0 ± 0.4	144 ± 24
EKE-AAA (E1013A/K1014A/E1015A)	879 ± 31	650 ± 21	54	220 ± 6	7.2 ± 0.20	121 ± 4
GG-AA (G1009A/G1010A)	850 ± 45	532 ± 29	58	446 ± 39	3.3 ± 0.2	136 ± 17
P1008A	722 ± 35	411 ± 15	ND	441 ± 28	2.9 ± 0.1	155 ± 7
R935A	558 ± 5	2045 ± 77	84	299 ± 18	2.4 ± 0.2	232 ± 17
R936A	660 ± 14	647 ± 27	ND	321 ± 11	2.7 ± 0.1	149 ± 8
K768A	430 ± 11	2105 ± 50	45	40 ± 2	39.2 ± 1.4	876 ± 52
K768M	722 ± 47	1449 ± 52	ND	120 ± 3	8.1 ± 0.3	191 ± 10

[a] Data are from Fig. 2 or were obtained from similar experiments with the remaining mutants.
[b] Data are from Fig. 3 or were obtained from similar experiments with the remaining mutants.
[c] These values represent the amplitude of the slow phase corresponding to the fitted curves in Fig. 5; the Na^+ concentration is 150 mM.
[d] Data are from Fig. 8 or were obtained from similar experiments with the remaining mutants.
[e] Data are from Fig. 9 or were obtained from similar experiments with the remaining mutants.
[f] These values represent the $K_{0.5}$ value for inhibition of the Na^+,K^+-ATPase activity by ouabain. The Na^+,K^+-ATPase activity was determined at 37 °C in 30 mM histidine buffer (pH 7.4), 130 mM NaCl, 20 mM KCl, 3 mM ATP, 3 mM $MgCl_2$, 1 mM EGTA, and various concentrations of ouabain. A function with the ouabain-inhibited enzyme represented by the sum of two hyperbolic components ($V = V_{tot} - a_1[ouabain]/(K_1 + [ouabain]) - a_2[ouabain]/(K_2 + [ouabain])$), a high affinity component corresponding to endogenous COS-1 cell Na^+,K^+-ATPase and a low affinity component corresponding to recombinant exogenous rat Na^+,K^+-ATPase, was fitted to the data. The $K_{0.5}$ value determined for the endogenous enzyme was ≤1.0 μM.
[g] del, deletion.
[h] ND, not determined.
[i] ΔKETYY has been previously studied (4), and the $K_{0.5}$ values for Na^+, ATP, and vanadate are the same as reported in Ref. 4.

a triple mutation replacing these three charged residues by alanines. The residues in the preceding loop, Pro^{1008}, Gly^{1009}, and Gly^{1010}, were likewise examined by alanine substitutions. The two C-terminal tyrosines were examined by single and double replacements with alanine removing the aromatic function, and to study the importance of the phenolic hydroxyl groups, each of the tyrosines was replaced with phenylalanine. The functional importance of the putative interactions of Arg^{935} with the C terminus (Fig. 1) was examined by substitution of Arg^{935} with alanine, and the juxtaposed Arg^{936} was likewise studied by replacement with alanine. The M5 residue Lys^{768} within interaction distance of the C terminus was replaced with both alanine and methionine, the latter to remove the positive charge but retain the bulk of the side chain.

Expression and Catalytic Turnover Rate—The mutations were introduced into the cDNA encoding the ouabain-resistant rat α_1-isoform of the Na^+,K^+-ATPase, and the wild-type and mutant rat enzymes were expressed using the mammalian COS-1 cell system under ouabain-selective pressure (8, 9). All the mutants were capable of sustaining cell growth in the presence of ouabain at a concentration inhibiting the endogenous COS-1 cell Na^+,K^+-ATPase, indicating that the Na^+ and K^+ transport rates of the mutants are sufficiently high to be compatible with cell viability.

The catalytic turnover rate (Na^+,K^+-ATPase activity per active site) measured at 130 mM Na^+, 20 mM K^+, and 3 mM ATP on the isolated membranes containing the expressed exogenous enzyme was markedly reduced for mutant K768A (2896 ± 179 min^{-1} ($n = 8$), compare with wild type 8474 ± 165 min^{-1} ($n = 11$)). A slight reduction relative to wild type was found for mutants R935A (6278 ± 311 min^{-1} ($n = 8$)) and ΔWVEKETYY (6556 ± 125 min^{-1} ($n = 6$)). For the remaining mutants there was no significant reduction of the catalytic turnover rate measured under these conditions (*e.g.* ΔYY 8059 ± 339 min^{-1} ($n = 8$) and YY-AA 9193 ± 614 min^{-1} ($n = 8$)). (See Table 1 for definitions of the multiple substitutions used in this study.)

K^+ Dependence—Fig. 2 shows the K^+ concentration dependence of the Na^+,K^+-ATPase activity at a relatively low Na^+ concentration of 40 mM. K^+ present at submillimolar concentrations activates ATP hydrolysis due to the stimulation of dephosphorylation by K^+ binding at the external sites on E_2P (*cf.* Scheme 1). All the mutants showed wild type-like (less than 2-fold deviation from wild type) apparent affinity for K^+ activation (Fig. 2 and Table 1). However, several of the mutants also displayed, in addition to the K^+ activation phase, an inhibition phase at high K^+ concentrations. This inhibition was particularly manifest (>20% inhibition) for the C-terminal deletion mutants ΔYY, ΔTYY, and ΔWVEKETYY as well as for YY-AA, R935A, and K768A. A less pronounced inhibition was seen for Y1017A, Y1018A, and K768M, whereas there was no inhibition of the wild type, ΔY, Y1017F, Y1018F, T1016A, R936A, P1008A, GG-AA, and EKE-AAA (Fig. 2). As demonstrated by Skou (13) in his pioneering first study on the Na^+,K^+ pump, such an inhibition phase can also be detected for the wild-type enzyme if the Na^+ concentration is lowered. This inhibition is caused by K^+ binding in competition with Na^+ at the cytoplasmically facing E_1 sites. The inhibition seen here for some of the mutants may therefore be caused by an increased ability of K^+ to compete with Na^+ at the E_1 sites.

Na^+ Dependence of Phosphorylation—To determine the Na^+ affinity at the cytoplasmically facing sites of the E_1 form, the Na^+ dependence of phosphorylation from [γ-^{32}P]ATP was

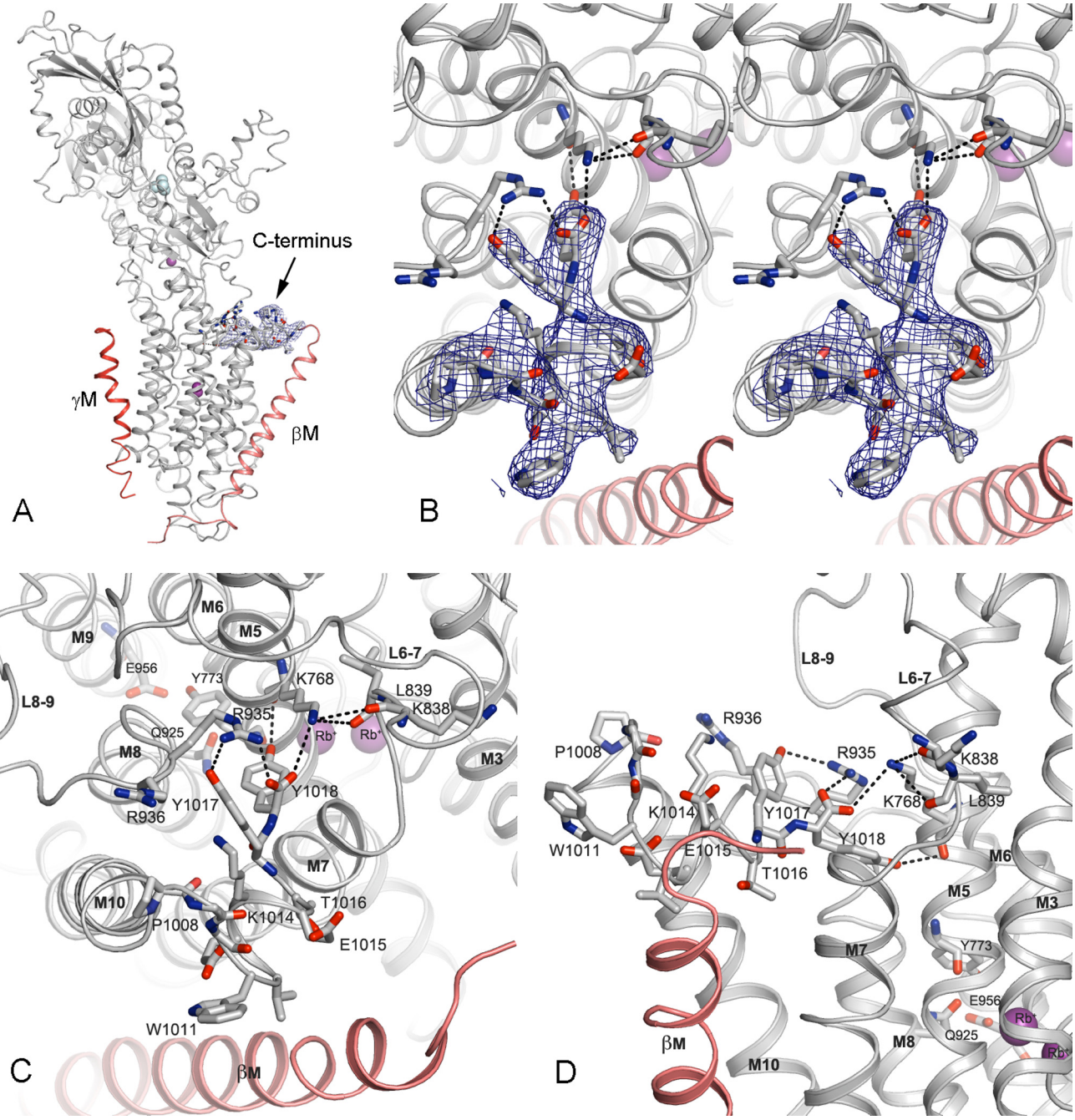

FIGURE 1. **Structural features of the C terminus in the crystallized $[K_2]E_2MgF$ form of the Na^+,K^+-ATPase.** The structure has Protein Data Bank (PDB) code 3B8E (4). The main chain of the α-subunit is *gray*, the β-subunit (membrane segment βM shown) is *purple*, and the γ-subunit (membrane segment γM shown) is *red*. *Pink spheres* indicate the two Rb^+ ions bound at the K^+ sites. Side chains of most of the residues considered in the present study are highlighted as *sticks*. Carbon atoms are indicated in *gray*, oxygen atoms in *red*, and nitrogen atoms in *blue*. *Dotted lines* indicate putative hydrogen bonds and salt links. *A*, overview of the structure, cytoplasmic side up. The *blue mesh* shows a $2F_o - F_c$ electron density map contoured at 1σ to cover the C-terminal residues. *B*, stereo view of the same electron density map of the C terminus as in *A* seen from the cytoplasmic side of the membrane. *C*, view from the cytoplasmic side of the membrane, showing details of the C terminus and its binding pocket as well as the putative third Na^+ binding site comprised by Tyr^{773}, Glu^{956}, and Gln^{925}. Residues highlighted as *sticks* are labeled with *numbers* according to the rat α_1-sequence. In addition, transmembrane helices M3, M5, M6, M7, M8, M9, and M10 and cytoplasmic loops L6–7 and L8–9 are labeled. *D*, side view along the membrane surface of the same details as in *C*.

studied in the absence of K^+, and in the presence of oligomycin added to stabilize the Na^+-occluded form as much as possible (Fig. 3). A 32-fold reduction of the Na^+ affinity relative to wild type was seen for YY-AA, and dramatic reductions were also found for the C-terminal deletion mutants ΔYY, ΔTYY, and ΔWVEKETYY (9-, 17-, and 25-fold, respectively, Fig. 3 and Table 1). The previously studied ΔKETYY mutant (4), giving a 26-fold reduction of Na^+ affinity for phosphorylation, fits nicely into this picture (data not shown here, but see summary in Table 1). It is noteworthy that the double substitution of the two terminal tyrosines with alanines, YY-AA, reduced the Na^+ affinity significantly more than deletion of the two tyrosines. A 5-fold reduction of Na^+ affinity was seen upon single alanine substitution of the most C-terminal tyrosine, Y1018A, whereas

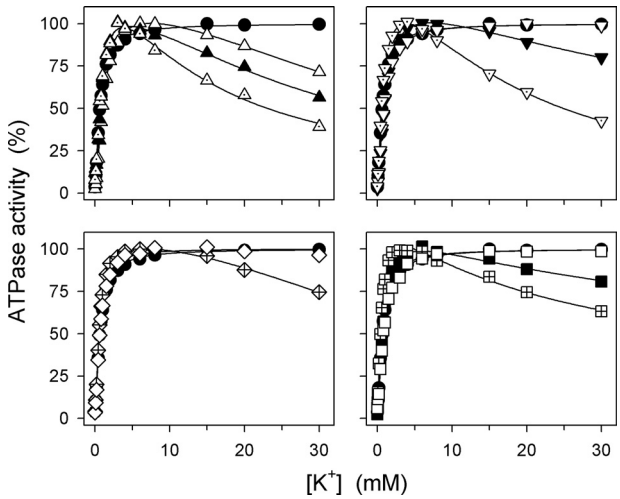

FIGURE 2. **K^+ dependence of Na^+,K^+-ATPase activity.** Measurements were performed at 37 °C in 30 mM histidine (pH 7.4), 40 mM NaCl, 3 mM ATP, 3 mM $MgCl_2$, 1 mM EGTA, 10 μM ouabain, and the indicated concentrations of K^+ added as KCl. *Filled circle*, wild type; *open triangle pointing upward*, ΔYY; *filled triangle pointing upward*, ΔTYY; *dotted triangle pointing upward*, ΔWVEKETYY; *open triangle pointing downward*, Y1018F; *filled triangle pointing downward*, Y1018A; *dotted triangle pointing downward*, YY-AA; *open diamond*, R936A; *crossed diamond*, R935A; *open square*, EKE-AAA; *filled square*, K768M; *crossed square*, K768A. For comparison, the wild type is shown in all panels. The $K_{0.5}(K^+)$ values for the activating phase are indicated in Table 1.

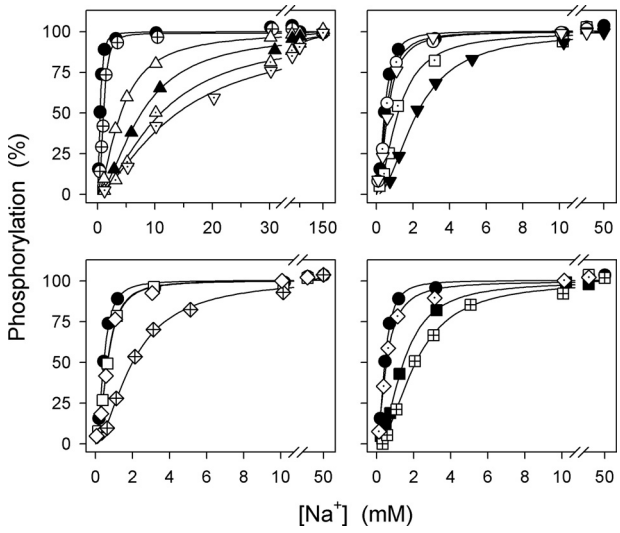

FIGURE 3. **Na^+ dependence of phosphorylation by ATP.** Phosphorylation was carried out for 10 s at 0 °C in 20 mM Tris (pH 7.5), 3 mM $MgCl_2$, 2 μM [γ-^{32}P]ATP, 10 μM ouabain, 20 μg/ml oligomycin, and the indicated concentrations of Na^+ added as NaCl with varying amounts of *N*-methyl-D-glucamine to maintain the ionic strength. *Filled circle*, wild type; *crossed circle*, ΔY; *open triangle pointing upward*, ΔYY; *filled triangle pointing upward*, ΔTYY; *dotted triangle pointing upward*, ΔWVEKETYY; *dotted triangle pointing downward*, YY-AA; *dotted circle*, Y1017F; *open triangle pointing downward*, Y1018F; *dotted square*, Y1017A; *filled triangle pointing downward*, Y1018A; *open square*, EKE-AAA; *open diamond*, R936A; *crossed diamond*, R935A; *dotted diamond*, GG-AA; *filled square*, K768M; *crossed square*, K768A. For comparison, the wild type is shown in all panels. Each *line* shows the best fit of the Hill equation, and the extracted $K_{0.5}(Na^+)$ values are indicated in Table 1.

2.7- and 2.3-fold reductions were seen for alanine substitution of the preceding tyrosine, Y1017A, and deletion of a single tyrosine, ΔY, respectively. Removal of the side chain hydroxyl group from each of the tyrosines by replacement with phenylalanine did not affect Na^+ affinity significantly (mutants Y1017F and Y1018F), and the same was the case for the mutations T1016A,

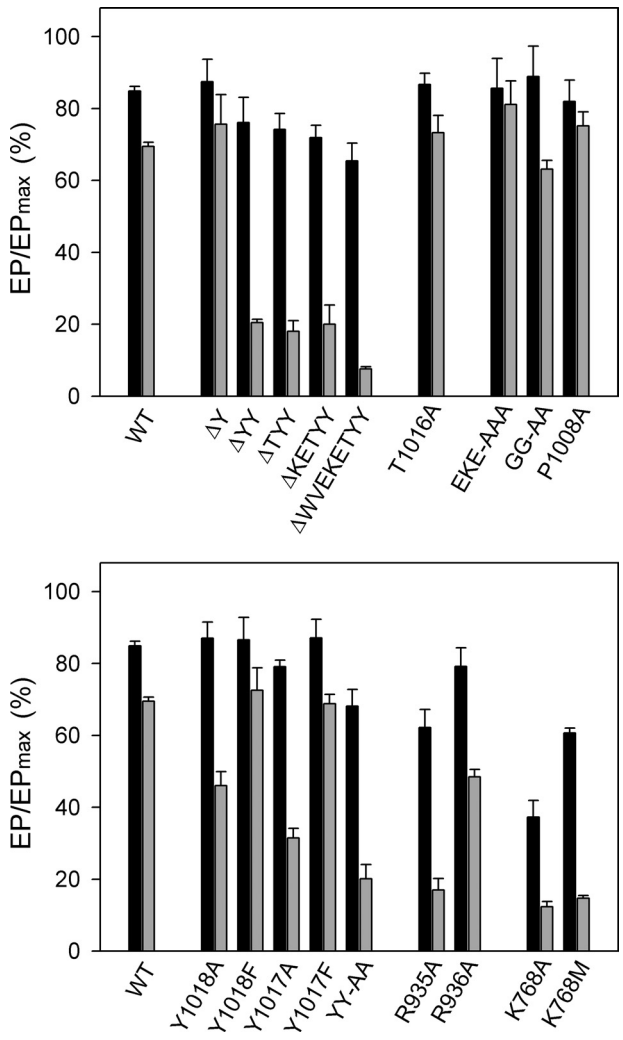

FIGURE 4. **Phosphorylation levels at 150 mM and 600 mM Na^+ relative to the maximum level obtained in the presence of oligomycin.** Phosphorylation was carried out for 10 s at 0 °C in 20 mM Tris (pH 7.5), 3 mM $MgCl_2$, 1 mM EGTA, 10 μM ouabain, 2 μM [γ-^{32}P]ATP, and 150 (*black columns*) or 600 (*gray columns*) mM NaCl. The phosphorylation level is shown relative to that obtained at 150 mM NaCl in the presence of oligomycin (20 μg/ml). Standard errors are indicated by *error bars*. *WT*, wild type.

R936A, P1008A, GG-AA, and EKE-AAA, whereas R935A reduced Na^+ affinity 5-fold. A 5-fold reduction was also seen for K768A, and a smaller, 3.3-fold reduction was seen for K768M (Fig. 3 and Table 1). These results correlate very well with the inhibitory effects of high K^+ concentrations seen in Fig. 2, the mutants with the most pronounced inhibition by K^+ also showing the largest reduction of Na^+ affinity, thus indicating that the enhanced ability of K^+ to compete with Na^+ in the E_1 form is caused by a weaker Na^+ binding at one or more of the E_1 sites.

Oligomycin Effect on Phosphoenzyme Level—Because oligomycin stabilizes the Na^+-occluded state (14, 15), thereby promoting phosphorylation and reducing dephosphorylation by blocking the $E_1P \rightarrow E_2P$ transition, the phosphoenzyme builds up to a maximal level in the presence of oligomycin. Fig. 4 shows the amount of phosphoenzyme accumulated in the absence of oligomycin, relative to the maximal phosphorylation level observed in the presence of oligomycin as stabilizer

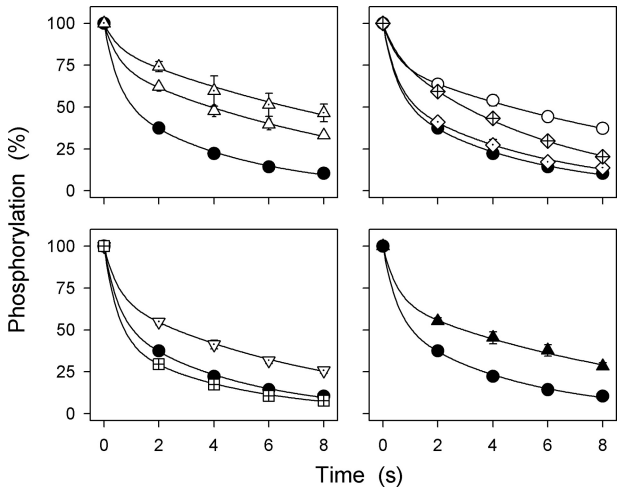

FIGURE 5. **Distribution of phosphoenzyme between E_1P and E_2P intermediates at 150 mM Na^+.** Phosphorylation was carried out for 10 s at 0 °C in 20 mM Tris (pH 7.5), 150 mM NaCl, 3 mM $MgCl_2$, 1 mM EGTA, 2 μM [γ-^{32}P]ATP, and 10 μM ouabain. Dephosphorylation was followed at 0 °C upon the addition of 2.5 mM ADP and 1 mM ATP. A biexponential function was fitted to the data, and the extent of the slow component, corresponding to the fraction of phosphoenzyme that is ADP-insensitive E_2P is indicated in Table 1 (E_2P). *Filled circle*, wild type; *dotted triangle pointing upward*, ΔWVEKETYY; *open triangle pointing upward*, ΔYY; *open circle*, ΔKETYY; *crossed diamond*, R935A; *dotted diamond*, GG-AA; *dotted triangle pointing downward*, YY-AA; *crossed square*, K768A; *filled triangle pointing upward*, ΔTYY. Standard errors are shown by *error bars* where larger than the size of the symbols.

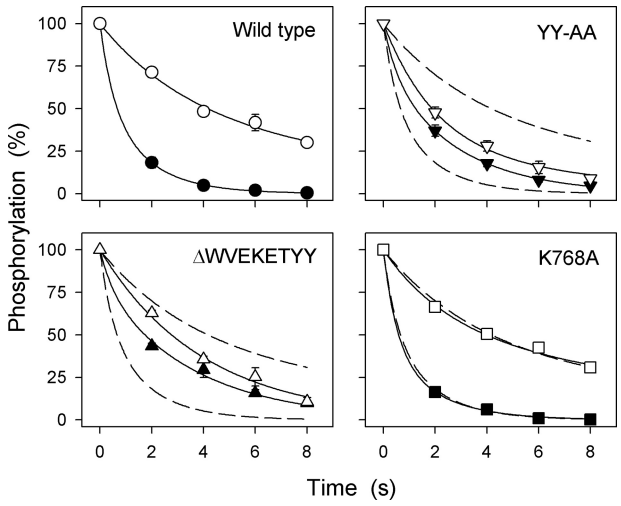

FIGURE 6. **Dephosphorylation with (*filled symbols*) and without (*open symbols*) ADP at 600 mM Na^+.** Phosphorylation was carried out for 10 s at 0 °C in 20 mM Tris (pH 7.5), 150 mM NaCl, 3 mM $MgCl_2$, 1 mM EGTA, 2 μM [γ-^{32}P]ATP, and 10 μM ouabain. Dephosphorylation was followed at 0 °C upon the addition of NaCl to give a final Na^+ concentration 600 mM and 1 mM ATP with 2.5 mM ADP (*filled symbols*) or 1 mM ATP without ADP (*open symbols*). The *broken lines* represent the wild-type data from the *upper left panel*. Standard errors are shown by *error bars* where larger than the size of the symbols.

(EP/EP$_{max}$ ratio), at two Na^+ concentrations of 150 and 600 mM. For the wild type, the EP/EP$_{max}$ ratio was 85 and 69% at 150 and 600 mM Na^+, respectively, and for most mutants, EP/EP$_{max}$ was wild type-like at 150 mM Na^+. Only K768A showed a marked reduction of EP/EP$_{max}$ to 37% under these conditions. At 600 mM Na^+, the mutants ΔYY, ΔTYY, ΔWVEKETYY, YY-AA, R935A, K768A, and K768M all showed a conspicuous reduction of EP/EP$_{max}$ to 20% or less. For comparison, we included the previously described ΔKETYY mutant (4), and this mutant showed a reduction of the EP/EP$_{max}$ ratio to the same low level at 600 mM Na^+ (Fig. 4). The low EP/EP$_{max}$ ratios may be the result of either a reduced phosphorylation rate or an increased dephosphorylation rate (see further under "Discussion").

Distribution of Phosphoenzyme between E_1P and E_2P at 150 mM Na^+—The two phosphoenzyme intermediates, E_1P and E_2P, are distinguished by difference in reactivity with ADP. The E_1P intermediate, which has three Na^+ ions bound in an occluded state, is ADP-sensitive, *i.e.* able to react with ADP and donate the phosphoryl group back to ADP, forming ATP. By contrast, E_2P is ADP-insensitive but dephosphorylates by hydrolysis of the aspartyl phosphoryl bond. The latter reaction is activated by K^+, binding with high affinity at two extracellularly facing sites on E_2P (Scheme 1), and to some extent by Na^+, presumably binding at the same sites as K^+ but with low affinity (3). Upon the addition of ADP to the phosphoenzyme formed from [γ-^{32}P]ATP, two decay phases can be distinguished, a rapid phase corresponding to E_1P reacting backward with ADP and a slow phase corresponding to decay of E_2P (10–12). Fig. 5 shows the results of such ADP dephosphorylation experiments carried out with selected mutants following phosphorylation with [γ-^{32}P]ATP in the absence of oligomycin (to allow subsequent dephosphorylation) and in the presence of 150 mM Na^+ (to obtain a sufficiently high phosphorylation level for the dephosphorylation rate to be accurately determined, *cf.* Fig. 4). The relative amounts of the rapidly and slowly dephosphorylating components were determined by fitting a biexponential function, and the amplitude of the slow phase (E_2P) is indicated in Table 1. The mutants ΔYY, ΔTYY, ΔKETYY, ΔWVEKETYY, YY-AA, and R935A, displaying a large reduction in affinity for cytoplasmic Na^+ (Fig. 3), also exhibited a higher E_2P level (68–85%) than wild type (57%). Mutant K768A exhibited a lower E_2P level (45%) than the wild type, *i.e.* an increased amount of ADP-sensitive E_1P, and mutants EKE-AAA and GG-AA were wild type-like.

Na^+ Interaction at External Low Affinity Sites—Experiments measuring Na^+ flux and ADP-ATP exchange using sided Na^+,K^+-ATPase membrane preparations have established that Na^+ binds to intracellular activating sites as well as to extracellular inhibitory and activating sites (16–21). Na^+ is released at the extracellular side of the membrane in association with the conformational transition from E_1P to E_2P, and a high extracellular Na^+ concentration drives the E_1P → E_2P transition backwards, resulting in accumulation of E_1P that can be dephosphorylated by ADP (21, 22). To examine whether the increased E_2P fraction of the phosphoenzyme seen for some of the mutants at 150 mM Na^+ is caused by a reduced ability of the phosphoenzyme to bind extracellular Na^+, we studied the interaction of Na^+ with the extracellularly facing low affinity sites further in selected mutants, ΔWVEKETYY, YY-AA, and K768A. The time course of dephosphorylation was determined following the addition of a high NaCl concentration of 600 mM with and without ADP (Fig. 6). In the wild type, the high NaCl concentration leads to an acceleration of dephosphorylation in the presence of ADP, which dephosphorylates E_1P, and to a slowing of the dephosphorylation in the absence of ADP, where the dephosphorylation occurs exclusively by hydrolysis of E_2P. This

is due to the high Na^+ concentration promoting conversion of E_2P back to E_1P and is not an unspecific effect of high ionic strength or an effect caused by the high concentration of Cl^- because 150 mM NaCl together with 450 mM choline chloride was unable to convert E_2P back to E_1P to an extent comparable with that obtained in the presence of 600 mM NaCl (see supplemental Fig. S1). Fig. 6 shows that the phosphoenzyme of ΔWVEKETYY or YY-AA decayed faster in the absence of ADP and slower in the presence ADP, as compared with wild type. Hence, the difference between the dephosphorylation rates observed with and without ADP was much smaller for ΔWVEKETYY and YY-AA than for wild type. The ability of Na^+ to drive the $E_1P \rightarrow E_2P$ reaction backwards therefore seems to be significantly diminished in these mutants. A wild-type-like behavior was, on the other hand, seen for K768A in these experiments (Fig. 6), thus indicating that K768A interacts normally with extracellular Na^+.

The behavior of the extracellularly facing Na^+ sites was also examined in studies of the ATPase activity in the absence of K^+ (Na^+-ATPase, Fig. 7). Under these conditions, the maximal catalytic turnover rate is only a small percentage of that obtained in the presence of K^+ because Na^+ is much less efficient as an activator of E_2P dephosphorylation as compared with K^+ (3). Extracellular Na^+ at high concentrations ($K_{0.5}$ (ligand concentration giving half-maximum effect) 600–700 mM) inhibits the Na^+-ATPase activity of the wild type by displacing the E_1P-E_2P conformational equilibrium in favor of E_1P (21, 22). Again, this is a rather specific effect of Na^+ because choline chloride in the same concentration range exerted much less inhibition (see supplemental Fig. S2). Notably, the low affinity inhibition by Na^+ was completely abolished (at least up to 1 M Na^+) in mutants ΔYY, ΔTYY, ΔKETYY, ΔWVEKETYY, YY-AA, and R935A. Some of these mutants showed a unique tendency to biphasic behavior with a plateau around 500 mM Na^+ and a further rise of the ATPase activity in the highest Na^+ concentration range where the wild type becomes fully inhibited. Such a further rise was not seen for mutants ΔY, Y1017A, and Y1018A, but the inhibition at the highest Na^+ concentrations was clearly much less pronounced in these mutants than in the wild type. Mutants EKE-AAA, GG-AA, and R936A, on the other hand, showed a wild-type-like inhibition by Na^+, whereas K768A was inhibited at lower Na^+ concentrations than the wild type (Fig. 7). These data match very well the data for interaction with extracellular Na^+ obtained in the studies of dephosphorylation (Figs. 5 and 6). Except for K768A, there is also good correlation with the mutational effects on activation by Na^+ binding at the cytoplasmically facing high affinity sites (Fig. 3), thus indicating that Na^+ interaction is disturbed on both sides of the membrane.

The E_1-E_2 Equilibrium of the Dephosphoenzyme—Because a displacement of the equilibrium between the conformational states E_1 and E_2 in favor of the E_2 form, away from the Na^+ binding E_1 form, would indirectly reduce the apparent Na^+ affinity at the cytoplasmically facing sites, assays were carried out to characterize the E_1-E_2 equilibrium. ATP binds with high affinity to E_1 and with low affinity to E_2 and shifts the E_1-E_2 equilibrium in favor of E_1 (Scheme 1). Hence, the apparent affinity for ATP in the activation of Na^+,K^+-ATPase activity

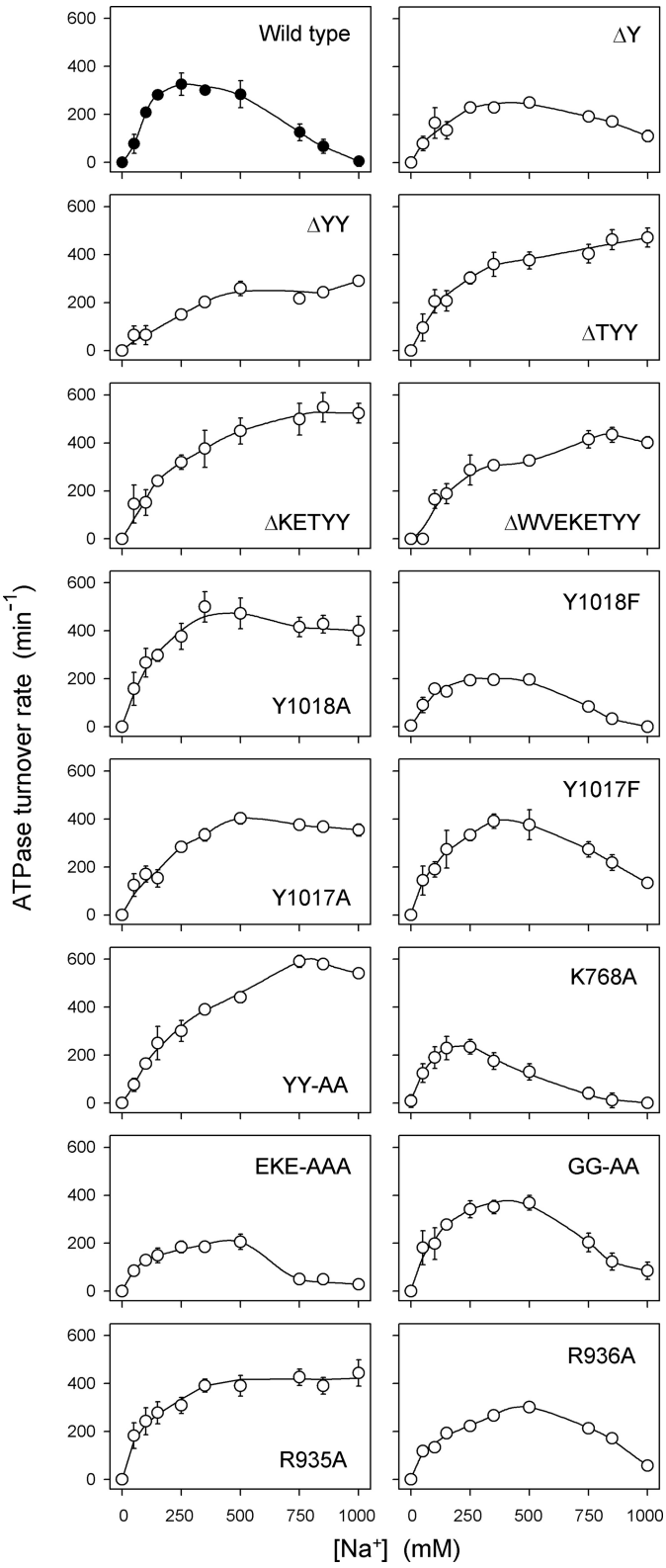

FIGURE 7. **Na^+ dependence of ATPase activity in the absence of K^+.** Na^+-ATPase activity was measured at 37 °C in 30 mM histidine (pH 7.4), 3 mM ATP, 3 mM $MgCl_2$, 1 mM EGTA, 10 μM ouabain, and the indicated concentrations of Na^+ added as NaCl. The molecular ATP hydrolysis activity (catalytic turnover rate) was calculated as the ratio between the specific ATPase activity and the active site concentration. Standard errors are shown by *error bars* where larger than the size of the symbols.

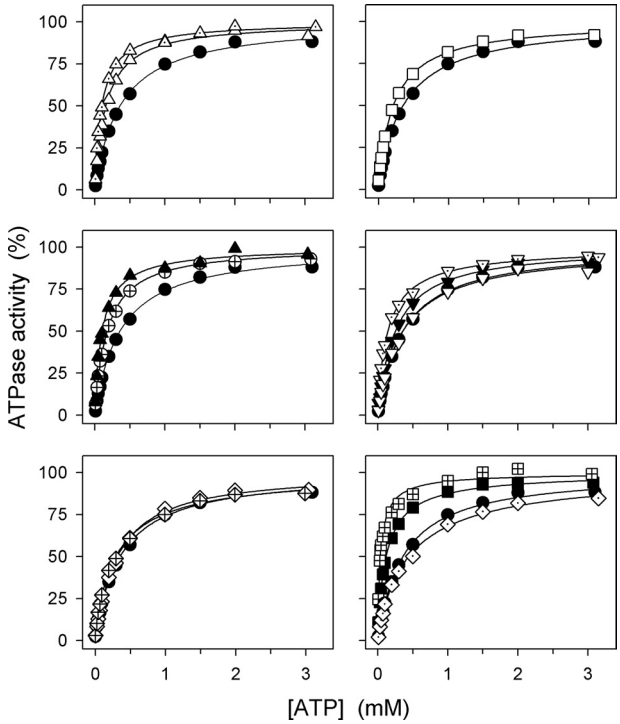

FIGURE 8. **ATP dependence of Na^+,K^+-ATPase activity.** The rate of ATP hydrolysis was determined at 37 °C in 30 mM histidine (pH 7.4), 130 mM NaCl, 20 mM KCl, 3 mM $MgCl_2$, 1 mM EGTA, 10 μM ouabain, and the indicated concentrations of ATP. *Filled circle*, wild type; *crossed circle*, ΔY; *open triangle pointing upward*, ΔYY; *filled triangle pointing upward*, ΔTYY; *dotted triangle pointing upward*, ΔWVEKETYY; *filled triangle pointing downward*, Y1018A; *dotted triangle pointing downward*, YY-AA; *open triangle pointing downward*, Y1018F; *open square*, EKE-AAA; *open diamond*, R936A; *crossed diamond*, R935A; *crossed square*, K768A; *filled square*, K768M; *dotted diamond*, GG-AA. For comparison, the wild type is shown in all panels. Each line shows the best fit of the Hill equation, and the extracted $K_{0.5}$(ATP) values are indicated in Table 1.

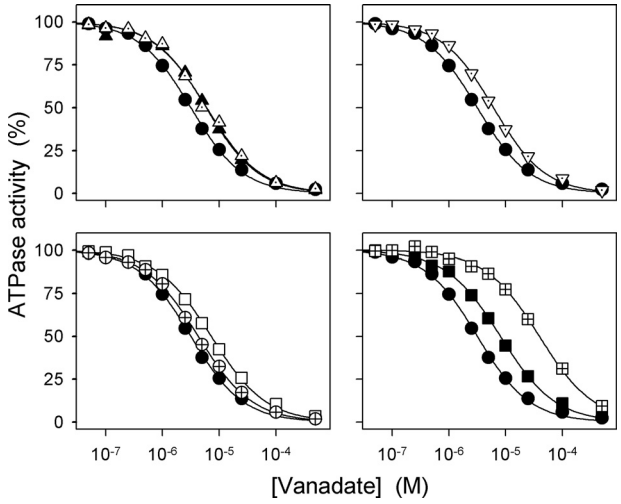

FIGURE 9. **Vanadate dependence of Na^+,K^+-ATPase activity.** The rate of ATP hydrolysis was determined at 37 °C in 30 mM histidine (pH 7.4), 130 mM NaCl, 20 mM KCl, 3 mM $MgCl_2$, 3 mM ATP, 1 mM EGTA, 10 μM ouabain, and the indicated concentrations of vanadate. *Filled circle*, wild type; *crossed circle*, ΔY; *filled triangle pointing upward*, ΔTYY; *dotted triangle pointing upward*, ΔWVEKETYY; *open square*, EKE-AAA; *crossed square*, K768A; *filled square*, K768M; *dotted triangle pointing downward*, YY-AA. Each line shows the best fit of the Hill equation, and the extracted $K_{0.5}$(vanadate) values for vanadate inhibition are indicated in Table 1.

should decrease if the E_1-E_2 equilibrium were displaced toward E_2 by the mutation (*cf.* Ref. 11). Fig. 8 and Table 1 show that the mutants with the most severe reduction of the apparent affinity for Na^+ (ΔYY, ΔTYY, ΔKETYY, ΔWVEKETYY, and YY-AA) on the contrary displayed an enhanced affinity for ATP consistent with a poise of the E_1-E_2 equilibrium in favor of E_1 rather than E_2. Likewise, EKE-AAA, ΔY, and the two Lys^{768} mutants showed an enhanced affinity for ATP; in particular, the ATP affinity of K768A was found as much as 9-fold increased relative to wild type. This mutant also showed a dramatic reduction of the apparent affinity for vanadate (12-fold) as inhibitor of the Na^+,K^+-ATPase activity (Fig. 9 and Table 1). Because vanadate binds to the E_2 form and not to E_1, the reduction of vanadate affinity supports the notion that the E_1-E_2 equilibrium is strongly shifted toward E_1 in mutant K768A. Less pronounced reductions of vanadate affinity were found for K768M, ΔTYY, ΔWVEKETYY, YY-AA, EKE-AAA, and ΔY in agreement with the smaller effect on ATP affinity. The remaining mutants including R935A showed little or no changes in affinities for ATP and vanadate, relative to wild type.

Ouabain is another inhibitor binding preferentially to the E_2 form (albeit with rather low affinity in the rat enzyme). As with vanadate, the affinity for ouabain was also significantly reduced (6-fold) in K768A relative to wild type (Table 1), again indicating a marked shift of the E_1-E_2 equilibrium in favor of E_1 in this mutant. Because the E_1-E_2 conformational equilibrium either is displaced in favor of E_1 or is wild type-like in the mutants studied here, the reduced affinity for Na^+ observed for several of the mutants is not an indirect effect caused by displacement of the conformational equilibrium in favor of E_2 but represents a "true" reduction of the intrinsic Na^+ affinity.

DISCUSSION

The C Terminus Controls Na^+ Affinity on Both Sides of the Membrane—The present data demonstrate that the C-terminal switch region of the Na^+,K^+-ATPase is involved in control of Na^+ affinity both on the cytoplasmic side and on the extracellular side of the membrane. The severely reduced affinity for Na^+ activation of phosphorylation (Fig. 3) and increased inhibition of Na^+,K^+-ATPase activity by high K^+ concentrations (Fig. 2) seen for several C-terminal mutations are indicative of defective Na^+ binding at cytoplasmically facing activating high affinity site(s) on the E_1 form of the enzyme. Na^+ interaction with one or more of the extracellularly facing sites appears to be disrupted as well in these mutants because Na^+ at a high concentration was unable to drive the $E_1P \rightarrow E_2P$ reaction backwards toward E_1P. Hence, 600 mM Na^+ did not inhibit dephosphorylation in the absence of ADP and was unable to promote ADP sensitivity of the phosphoenzyme (Fig. 6), and Na^+-ATPase activity remained maximally stimulated at the high Na^+ concentrations where the wild type is almost completely inhibited (Fig. 7). Thus, for at least one of the three transported Na^+ ions, the same structural elements seem to be involved in control of binding on either side of the membrane.

Interaction of Arg^{935} with the Two C-terminal Tyrosines Is of Crucial Importance for Na^+ Affinity—The effect on Na^+ affinity for activation of phosphorylation of E_1 seems to increase with increasing length of the deletion up to a certain point (ΔY, ΔYY, ΔTYY, ΔKETYY, and ΔWVEKETYY showing 2.3-, 9-,

17-, 26-, and 25-fold reduction of Na^+ affinity, respectively). Because alanine mutations of the EKE segment and the threonine (Thr^{1016}) contained within the α-helical part of WVEKETYY were without influence on the affinity for Na^+, side chain interactions of EKET do not seem to be of importance for Na^+ binding. Likewise, changes to the loop preceding the α-helix (mutations P1008A and GG-AA) did not affect Na^+ affinity. This clearly brings the two C-terminal tyrosines Tyr^{1017} and Tyr^{1018} into focus. The reason that the effects on Na^+ affinity of the longer deletions were even more pronounced than the 9-fold reduction seen for ΔYY could be that the C-terminal carboxylate group is involved in multiple interactions in this region (*cf.* Fig. 1) that are gradually interrupted by deletions of increasing length.

Alanine substitution of Arg^{935} likewise resulted in a significant 5-fold reduction of Na^+ affinity on the cytoplasmic side and lack of Na^+ inhibition of Na^+-ATPase activity indicative of disruption of Na^+ binding from the extracellular side. The Arg^{935} mutation therefore resembles the C-terminal deletions with respect to functional effects. By contrast, alanine substitution of the juxtaposed Arg^{936} was without influence on Na^+ affinity on either side of the membrane. These results fit well with the structure shown in Fig. 1, where Arg^{935} is in position to form one or two salt bridge/hydrogen bonds with the C-terminal carboxylate group (3.0 and 3.6 Å distance), whereas Arg^{936} points away from the C terminus.

It is notable that the double alanine substitution YY-AA is the mutation resulting in the largest reduction of apparent Na^+ affinity for activation of phosphorylation (32-fold), indicating that the presence of the alanine side chains is even more disturbing than removal of the two tyrosines by deletion. In fact, the 32-fold reduction of Na^+ affinity is larger than seen for substitution of some of the membrane-buried residues with oxygen-containing side chains known to interact with the transported cations (23, 24). The structure in Fig. 1 indicates that the side chain hydroxyl groups of the two terminal tyrosines are within hydrogen-bonding distance of the Arg^{935} side chain and the Lys^{768} main chain carbonyl group, respectively. However, our data for the Y1017F and Y1018F mutants show rather wild-type-like Na^+ affinity, in contrast to the 2.7–5-fold reduction of Na^+ affinity seen for the Y1017A and Y1018A mutants. Therefore, interactions of the hydroxyl groups of the two terminal tyrosines are of little importance for Na^+ binding and may not exist in the native enzyme, at least not in the Na^+-bound E_1 form. The effects of the alanine substitutions indicate, on the other hand, that the aromatic function plays a significant role. This could be through arginine-π interaction (stacking interaction between the cationic guanidinium functionality of arginine and the conjugated π-system of the tyrosine), which is common in proteins (25). In Fig. 1, the distances from the nitrogen atoms of the Arg^{935} side chain to the aromatic rings of Tyr^{1017} and Tyr^{1018} are 5.3 and 5.7 Å, respectively, thus clearly allowing arginine-π interaction to both rings with a minor adjustment of side chain conformation. This could be a particular feature of the E_1 form.

The C Terminus May Influence the Third Na^+ Site through Arg^{935}—An important challenge is to define the particular Na^+ site(s) controlled by the C terminus and the underlying mechanism. This is not simple because the binding of all three Na^+ ions being transported is needed for activation of phosphorylation of the E_1 form by ATP (26). The deocclusion/release of the three Na^+ ions toward the extracellular side occurs in distinct and sequential steps (Scheme 1), the release of the first Na^+ ion being electrogenic and slow, rate-limited by the $E_1P \rightarrow E_2P$ conformational transition (27, 28). If K^+ is absent, two Na^+ ions may rebind to E_2P at the externally facing K^+ sites to provide partial activation of E_2P dephosphorylation and inward Na^+ transport resulting in Na^+-Na^+ exchange coupled with Na^+-ATPase activity (1). It is of notice that the apparent K^+ affinity was wild type-like in the mutants with C-terminal changes, as well as in R935A (Fig. 2). Moreover, the activation of E_2P dephosphorylation by Na^+ binding at the K^+ sites appeared intact as judged from the high Na^+-ATPase activity and the direct measurements of dephosphorylation at 600 mM Na^+ in the two mutants with the most significant reduction of Na^+ affinity (ΔWVEKETYY and YY-AA; Fig. 6, *open symbols*). The residues binding the two K^+ ions in E_2P and E_2, and probably the Na^+ ions activating E_2P dephosphorylation, are more or less the same as those expected to bind two of the three Na^+ ions in E_1 ("site 1" and "site 2," see Refs. 4 and 29). Hence, our data would be in accordance with a model in which only the site binding the third Na^+ ion ("site 3") is under control of the C terminus, thus suggesting that the third Na^+ ion is particularly important for driving the $E_1P \rightarrow E_2P$ transition backwards. The Na^+ ion leaving first in the sequential release during the $E_1P \rightarrow E_2P$ transition could very well be the Na^+ ion bound at site 3, although this has yet to be definitively proven.

Among several residues suggested as putative ligands binding the Na^+ ion at site 3 (4, 29, 30, 31), Tyr^{773}, Gln^{925}, and Glu^{956} are most closely associated with the structural elements interacting with the C terminus (Fig. 1, *C* and *D*). On the basis of the present findings defining Arg^{935} as a crucial residue for control by the C terminus of Na^+ affinity on both sides of the membrane and the strategic position of Arg^{935} in the cytoplasmic loop between transmembrane helices M8 and M9 that contain Gln^{925} and Glu^{956}, it is conceivable that Arg^{935} forms a structural and functional link between the C terminus and the third Na^+ binding site.

The homologous arginine in the human α_2-isoform (Arg^{937}) has been found mutated to proline in patients with familial hemiplegic migraine type 2 (FHM2) (32). It seems likely that disruption of the link to the C terminus, in addition to a more rigid structure of the L8–9 loop due to the proline (33), causes the functional disturbance underlying the pathophysiology.

In addition to the low affinity extracellular Na^+ binding site(s) responsible for driving the $E_1P \rightarrow E_2P$ transition backwards and inhibiting Na^+-ATPase activity with a $K_{0.5}$ of 600–700 mM in the wild type, an inhibitory extracellular Na^+ site of high affinity ($K_{0.5} < 5$ mM) has also been described for certain enzyme preparations (3, 16–20). The plateau phase in the Na^+ dependence of Na^+-ATPase activity seen around 500 mM Na^+ for the C-terminal mutations with the largest reduction of cytoplasmic Na^+ affinity (Fig. 8) might be taken as an indication that the affinity of the high affinity inhibitory extracellular site is reduced in parallel with that of the low affinity extracellular site(s).

Furthermore, it is worth noting that the apparent binding affinities of the extracellular Na^+ sites and the E_1P-E_2P equilibrium vary among isoforms as well as species and tissues (21, 34–36), indicating that non-conserved residues not studied here, the specific lipid environment, and/or interaction with regulatory proteins contribute to determine the effect of extracellular Na^+. Such influence might in some cases be mediated through changes in the interactions of the C terminus.

Roles of Lys^{768}—Like R935A, the K768A mutant exhibited a significant 5-fold reduction of Na^+ affinity for activation of phosphorylation, which would be explained if the side chain amino group of Lys^{768} contributes to the positioning of the C terminus through interaction with the carboxylate group (the 4.1 Å distance in the E_2 structure in Fig. 1 might well be shorter in the Na^+-bound E_1 conformation). The interaction of Lys^{768} with the C-terminal carboxylate might also influence the position of M5, which could contribute to determine the affinity of the third Na^+ site through the M5 residue Tyr^{773} (Fig. 1), a crucial residue for Na^+ binding but not for K^+ binding (37). That the methionine substitution K768M gives a smaller 3.3-fold reduction of Na^+ affinity makes sense in this context because the methionine side chain has some hydrogen-bonding potential, thus possibly being able to partially substitute for the lysine.

By contrast, the K768A mutant behaved markedly different from the mutants with C-terminal changes as regards the binding of Na^+ at the inhibitory/release site(s) facing the external side. Hence, in K768A, high Na^+ concentrations promoted accumulation of E_1P to at least the same extent as in the wild type (Figs. 5 and 6), and K768A was very sensitive to inhibition of Na^+-ATPase activity by Na^+ (Fig. 7). Thus, Lys^{768} does not seem to be required for binding of Na^+ from the extracellular side, which could mean that the $E_1P \rightarrow E_2P$ transition weakens the interaction of Lys^{768} with the C terminus. Because the E_1-E_2 conformational equilibrium of the dephosphoenzyme was much more strongly displaced toward E_1 in K768A than seen for any of the other mutants, the Lys^{768} side chain must have a very important role in stabilizing the E_2 form and likely also in stabilizing E_2P. We speculate that the stabilization of E_2/E_2P is mediated by bonds formed with the main chain carbonyl groups of Lys^{838} and Leu^{839} in the cytoplasmic loop between transmembrane segments M6 and M7 ("L6–7 loop," Fig. 1; the distances from Lys^{768} to the main chain carbonyl groups of Lys^{838} and Leu^{839} are 3.6 and 4.0 Å, respectively). It is possible that in the wild-type Na^+,K^+-ATPase, the bonds between Lys^{768} and L6–7 are weakened in connection with the E_2 to E_1 conformational transition, which would explain that breakage of these bonds by substitution of the lysine leads to a relative destabilization of E_2 and thereby to displacement of the E_1-E_2 equilibrium in favor of E_1. Hence, in the wild type, the side chain of Lys^{768} might shift its bonding pattern from interaction with L6–7 in E_2 forms to strengthening of the bond with the C terminus in E_1 forms.

The K768A mutant moreover showed markedly lower accumulation of phosphoenzyme in the presence of 150 mM Na^+ without oligomycin (EP/EP_{max} of K768A only 37%, Fig. 4, *black columns*) as compared with the mutants with C-terminal changes. At 600 mM Na^+, on the other hand, all the mutants with significantly reduced Na^+ affinity behaved similarly, displaying an EP/EP_{max} ratio <20% (Fig. 4, *gray columns*). For the mutants with C-terminal changes as well as R935A, the low EP/EP_{max} seen at 600 mM Na^+ can be understood as a consequence of the increased rate of dephosphorylation caused by inability of the Na^+ ion(s) to drive the $E_1P \rightarrow E_2P$ reaction backwards toward E_1P in combination with a normal ability of Na^+ at high concentrations to activate dephosphorylation of E_2P by binding at the two externally facing K^+ sites. By stabilizing the E_1P form, oligomycin is able to counteract the increased rate of dephosphorylation. For these mutants, it is therefore not necessary to assume that the phosphorylation rate differs significantly from that of the wild type at saturating Na^+ concentrations. For K768A, the situation is different because the $E_1P \rightarrow E_2P$ reaction is driven backwards toward E_1P by high Na^+ concentrations to at least the same extent as in the wild type (Fig. 6). The low EP/EP_{max} ratio in this mutant can therefore not be explained by an increased rate of dephosphorylation but must be due to a reduced rate of phosphorylation, relative to wild type, which would also explain the significant reduction of the catalytic turnover rate (to 33% of wild type) detected solely for this mutant. Because the Na^+ concentrations applied in the experiments corresponding to Fig. 4 are manyfold higher than the $K_{0.5}$ for Na^+ activation of phosphorylation ($K_{0.5}(Na^+) = 2.1$ mM, Table 1), it is likely that the maximal phosphorylation rate reached at saturating Na^+ is reduced in this mutant. This would be expected if Na^+ occlusion were defective because Na^+ occlusion is associated with enzyme conformational changes that are propagated to the catalytic site, thereby controlling the rate of phosphoryl transfer from ATP (15). By stabilizing the Na^+-occluded E_1 form, oligomycin would counteract the reduced rate of phosphorylation and allow a higher level of steady-state phosphorylation, exactly as observed. The defective Na^+ occlusion/reduced rate of phosphorylation and marked shift of the E_1-E_2 conformational equilibrium in favor of E_1 in the K768A mutant resemble the behavior exhibited by the previously characterized mutant with glutamine substitution of Glu^{329}, which is an essential gating residue in the cation binding pocket (4, 24). These features of the K768A mutant, which distinguish it from the mutants with low Na^+ affinity on both sides of the membrane, suggest that the bond between M5 and the C terminus through Lys^{768} is particularly important for stabilization of the Na^+-occluded state and/or the coupling between events in the cation binding pocket and the phosphorylation site.

Conclusion and Perspectives—Our data reveal structure-function relationships of importance for understanding the effects of the C terminus on Na^+ binding. We suggest that these effects involve the third Na^+ site and that Arg^{935} constitutes an important link between the C terminus and the third Na^+ site in its cytoplasmically facing as well as in its externally facing configuration. Arg^{935} likely interacts with the aromatic rings of the two C-terminal tyrosines. Lys^{768} may interact preferentially with the C terminus in E_1 and E_1P forms and with the L6–7 loop in E_2 and E_2P forms and is therefore only of importance for Na^+ binding from the cytoplasmic side and for Na^+ occlusion.

Our finding that the C terminus controls not only the affinity for Na^+ on the cytoplasmic side of the membrane but

also the affinity for Na^+ binding from the extracellular side driving the $E_1P \rightarrow E_2P$ transition backwards has bearings on the classic dispute as to whether ion pumps function as gated channel-like structures in which the ions diffuse between at least two sites in the transport pathway or as alternating access machines in which the same ion binding site opens consecutively to the cytoplasmic and the extracellular side (38). At least the Na^+ site being controlled by the C terminus now appears able to reorient such that it can face either side of the membrane alternatively. Of course, this does not exclude the presence of access channels that connect the binding site with the membrane surfaces. We speculate that the C terminus may constitute a central element of the mechanism that reorients the site.

Acknowledgments—We thank Kirsten Lykke Pedersen, Janne Petersen, Jytte Jørgensen, and Nina Juste for expert technical assistance.

REFERENCES

1. Glynn, I. M. (1993) *J. Physiol.* **462,** 1–30
2. Kaplan, J. H. (2002) *Annu. Rev. Biochem.* **71,** 511–535
3. Post, R. L., Hegyvary, C., and Kume, S. (1972) *J. Biol. Chem.* **247,** 6530–6540
4. Morth, J. P., Pedersen, B. P., Toustrup-Jensen, M. S., Sørensen, T. L., Petersen, J., Andersen, J. P., Vilsen, B., and Nissen, P. (2007) *Nature* **450,** 1043–1049
5. Toyoshima, C., Nakasako, M., Nomura, H., and Ogawa, H. (2000) *Nature* **405,** 647–655
6. Lutsenko, S., and Kaplan, J. H. (1993) *Biochemistry* **32,** 6737–6743
7. Geering, K. (2006) *Am. J. Physiol. Renal. Physiol.* **290,** F241–F250
8. Vilsen, B. (1992) *FEBS Lett.* **314,** 301–307
9. Jewell, E. A., and Lingrel, J. B. (1991) *J. Biol. Chem.* **266,** 16925–16930
10. Vilsen, B. (1997) *Biochemistry* **36,** 13312–13324
11. Toustrup-Jensen, M., Hauge, M., and Vilsen, B. (2001) *Biochemistry* **40,** 5521–5532
12. Rodacker, V., Toustrup-Jensen, M., and Vilsen, B. (2006) *J. Biol. Chem.* **281,** 18539–18548
13. Skou, J. C. (1957) *Biochim. Biophys. Acta.* **23,** 394–401
14. Esmann, M., and Skou, J. C. (1985) *Biochem. Biophys. Res. Commun.* **127,** 857–863
15. Skou, J. C. (1991) in *The Sodium Pump: Recent Developments* (Kaplan, J. H., and De Weer, P., eds) pp 317–319, The Rockefeller University Press, New York
16. Garrahan, P. J., and Glynn, I. M. (1967) *J. Physiol.* **192,** 159–174
17. Glynn, I. M., and Karlish, S. J. D. (1976) *J. Physiol.* **256,** 465–496
18. Beaugé, L. A., and Glynn, I. M. (1979) *J. Physiol.* **289,** 17–31
19. Kaplan, J. H. (1982) *J. Gen. Physiol.* **80,** 915–937
20. Kaplan, J. H., and Hollis, R. J. (1980) *Nature* **288,** 587–589
21. Yoda, S., and Yoda, A. (1986) *J. Biol. Chem.* **261,** 1147–1152
22. Taniguchi, K., and Post, R. L. (1975) *J. Biol. Chem.* **250,** 3010–3018
23. Vilsen, B. (1995) *Biochemistry* **34,** 1455–1463
24. Vilsen, B., and Andersen, J. P. (1998) *Biochemistry* **37,** 10961–10971
25. Gallivan, J. P., and Dougherty, D. A. (1999) *Proc. Natl. Acad. Sci. U.S.A.* **96,** 9459–9464
26. Schneeberger, A., and Apell, H. J. (1999) *J. Membr. Biol.* **168,** 221–228
27. Holmgren, M., Wagg, J., Bezanilla, F., Rakowski, R. F., De Weer, P., and Gadsby, D. C. (2000) *Nature* **403,** 898–901
28. Wuddel, I., and Apell, H. J. (1995) *Biophys. J.* **69,** 909–921
29. Ogawa, H., and Toyoshima, C. (2002) *Proc. Natl. Acad. Sci. U.S.A.* **99,** 15977–15982
30. Li, C., Capendeguy, O., Geering, K., and Horisberger, J. D. (2005) *Proc. Natl. Acad. Sci. U.S.A.* **102,** 12706–12711
31. Imagawa, T., Yamamoto, T., Kaya, S., Sakaguchi, K., and Taniguchi, K. (2005) *J. Biol. Chem.* **280,** 18736–18744
32. Riant, F., De Fusco, M., Aridon, P., Ducros, A., Ploton, C., Marchelli, F., Maciazek, J., Bousser, M. G., Casari, G., and Tournier-Lasserve, E. (2005) *Hum. Mutat.* **26,** 281
33. Morth, J. P., Poulsen, H., Toustrup-Jensen, M. S., Schack, V. R., Egebjerg, J., Andersen, J. P., Vilsen, B., and Nissen, P. (2009) *Phil. Trans. R. Soc. B.* **364,** 217–227
34. Kaplan, J. H., and Kenney, L. J. (1985) *J. Gen. Physiol.* **85,** 123–136
35. Therien, A. G., Nestor, N. B., Ball, W. J., and Blostein, R. (1996) *J. Biol. Chem.* **271,** 7104–7112
36. Crambert, G., Hasler, U., Beggah, A. T., Yu, C., Modyanov, N. N., Horisberger, J. D., Lelièvre, L., and Geering, K. (2000) *J. Biol. Chem.* **275,** 1976–1986
37. Vilsen, B., Ramlov, D., and Andersen, J. P. (1997) *Ann. N.Y. Acad. Sci.* **834,** 297–309
38. Läuger, P. (1991) *Electrogenic Ion Pumps*, pp. 27–32, Sinauer Associates, Sunderland, MA